Available online at www.sciencedirect.com
ScienceDirect
Dyes and Pigments 75 (2007) 693–700
DYES and PIGMENTS
www.elsevier.com/locate/dyepig

Colored films produced by electron beam deposition from nanometric TiO_2 and Al_2O_3 pigment powders obtained by modified polymeric precursor method

M.I.B. Bernardi [a,*], F.S. De Vicente [a], M. Siu Li [b], A.C. Hernandes [a]

[a] *Grupo Crescimento de Cristais e Materiais Cerâmicos, Instituto de Física de São Carlos, Universidade de São Paulo, PO Box: 369, 13560-970 São Carlos, SP, Brazil*

[b] *Grupo de Fotônica, Instituto de Física de São Carlos, Universidade de São Paulo, PO Box: 369, 13560-970 São Carlos, SP, Brazil*

Received 21 February 2006; received in revised form 19 April 2006; accepted 26 July 2006
Available online 10 October 2006

Abstract

Synthesis and the characterization of TiO_2:5%Co (green), TiO_3:5%Fe (brown-reddish), TiO_2:2%Cr (brown), Al_2O_3:5%Co (blue), Al_2O_3:5%Fe (brown-reddish) and Al_2O_3:2%Cr (light green) nanometric pigment powders using polymeric precursor (modified Pechini's method) is reported. Colored thick films were deposited on amorphous quartz substrates by electron beam physical vapor deposition (EB-PVD) using pellets of the pigment powders as target. The evaporation process was carried out in vacuum of 4×10^{-6} Torr and the amorphous quartz substrates were kept at 350 °C during deposition. The TiO_2-based pigment powders presented crystalline anatase phase and the Al_2O_3-based pigment powders showed corundum phase, investigated by X-ray diffraction (XRD). The average particle size of the pigment powders was about 20 nm, measured by scanning electron microscopy with field emission gun (SEM-FEG). Diffuse reflectance spectra and colorimetric coordinates L^*, a^*, b^* using the CIE-$L^*a^*b^*$ method are shown for the pigment powders, in the 350–750 nm range. The colored thick films were characterized by transmittance (UV–Vis) and atomic force microscopy (AFM). The average film roughness was ~5.5 nm and the average grain size obtained in the films was around 75 nm. Films with thickness from 400 nm to 690 nm were obtained, measured by talystep profiler. Transmission spectra envelop method has been used to obtain refractive index and thickness of the Al_2O_3 colored thick films.

Keywords: Al_2O_3; TiO_2; Nanometric pigment powders; Polymeric precursor method; Thick films; Electron beam deposition

1. Introduction

Nanoscience is currently enabling revolutionary changes in several areas of technology but new paradigms will eventually have a much wider and innovative impact [1–3]. In the area of coatings and pigments, new approaches through nanoscale effects can be used to create coatings with significantly optimized properties. The conventional areas of its application are paints, building materials, plastics, enamel and ceramics [4]. The pigment materials used for these purposes are normally prepared at high temperatures and consist of powders with large particle sizes. However, for special applications such as coloring and UV-stabilization of plastics, inks, transparent thin films on glass, and coatings on luminescent materials, pigment particles in the nanoscale region are required. In view of this requirement, the preparation of nanometric pigment powders is considerably complicated by the unfavorable surface-to-volume ratio of the particles. It is necessary use for the low temperatures during the synthesis of pigments powders in order to limit the growth of particles that renders this situation even more difficult. In fact, nanometric oxide materials have been prepared at low temperatures by various methods [5–11], but the color quality of nanoscale materials has attracted only little attention up to now.

* Corresponding author. Tel.: +55 16 3739828; fax: +55 16 3739824.
E-mail address: m.basso@if.sc.usp.br (M.I.B. Bernardi).

0143-7208/$ - see front matter © 2006 Elsevier Ltd. All rights reserved.
doi:10.1016/j.dyepig.2006.07.022

Coating manufacturers consume nearly three million tonnes of TiO_2 pigments every year, a clear indication of the importance of this opacifying pigment. This reflects the high ability of TiO_2 to uniformly scatter white light without absorption (which would lead to color). In addition, TiO_2 possesses a number of attractive properties, among which are its high refractiveness, high dielectric constant, semiconductor properties and chemical stability. Compact TiO_2 thin films deposited on conducting glass are used in new types of liquid and solid dye-sensitized solar cells, as well as in solar cells with extremely thin organic or inorganic absorbers. These thin films are also of interest for application in the photo-oxidation of water, photocatalysis, and electrochromic devices [12].

Corundum (α-Al_2O_3) is one of the widely applied material in ceramics. Its extended use is due to low cost and important mechanical, electronic and catalytic properties [13]. In recent years, there has been an increasing interest in the synthesis of nanocrystalline Al_2O_3, which is important for a variety of applications including fabrication of metal ceramic laminate composites and as reinforcement phase in polymer and brittle matrix composites [14]. Conventional methods for synthesizing α-Al_2O_3 powder involve solid-state thermally driven transformations from the hydrates of aluminum oxide, and the total conversion to the corundum structure that occurs on heating above 1230 °C [15].

Several factors and characteristics should be considered in the selection of pigments for a specific application in ceramics. Most important of them are the intensity and the uniformity of the colors obtained as also the thermal stability and particle sizes of the powders. A method that has turned out to be quite advantageous in the preparation of nanoscale and crystalline oxide materials is the so-called Pechini's method [16]. The advantage of solution techniques is the quasi-atomic dispersion of the component cations in liquid precursors, which facilitates the synthesis of nanosize crystallized powder with high purity at low temperatures.

In this work is reported the preparation of TiO_2 and α-Al_2O_3-based pigment powders with nanometric particle sizes synthesized through a modified Pechini's method, using Cr, Co, and Fe as chromophore ions. Colored films were deposited on amorphous quartz substrates by electron beam deposition of pellets of the pigment powders. XRD, diffuse reflectance, colorimetric coordinates and SEM-FEG micrographs of the pigment powders are presented. UV–Vis transmittance spectra, AFM images of the grain size and roughness surface of the films were assessed.

2. Experimental

2.1. Nanometric TiO_2 and Al_2O_3 pigment preparation using modified Pechini's method

Pechini-type [2], in situ polymerisable complex methods are well known for the synthesis of homogenous bulk multi-component metal oxides. The method includes a combined process of metal complex formation and in situ polymerization of organics. The polymeric precursor method [17–19] consists of a process where ethylene glycol, citric acid, and metal ions are polymerized to form a polyester-type resin. The metal ions can be immobilized in a rigid polyester network leading to a reduced segregation during the processing. The metal sources used were $Ti[OCH(CH_3)_2]_4$ (Aldrich), $NH_4Al(SO_4)_2$ (Riedel), $Co(NO_3)_3 \cdot 9H_2O$ (Aldrich), $FeSO_4 \cdot 7H_2O$ (Becker), $Cr(NO_3)_3 \cdot 9H_2O$ (Aldrich), $HOCOH_2C(OH)(COOH)CH_2$-$COOH \cdot H_2O$ (citric acid – Synth), and $HOCH_2CH_2OH$ (ethylene glycol – Merck), all with P.A. degree. The source of aluminum was dissolved in ammonium hydroxide – NH_4OH – yielding aluminum hydroxide – $Al(OH)_3$ – according to Eq. (1):

$$NH_4Al(SO_4)_2 + 3NH_4OH \rightarrow Al(OH)_3 + (NH_4)_4(SO_4)_2 \quad (1)$$

After formation of the aluminum hydroxide precipitate, a paper filtering was made in order to completely eliminate the ammonium sulfate, by-product of the reaction. Controlled addition of citric acid, results in the formation of aluminum citrate and in the same way, the source of titanium was dissolved in citric acid to form the titanium citrate. Next was added the metallic cations Co (5 mol%), Fe (5 mol%), and Cr (2 mol%), which act as chromophore ions and the TiO_2 and Al_2O_3 act as opacifier agent. The citric acid/metal molar ratio and the citric acid/ethylene glycol mass ratio were 3:1 and 60/40, respectively. The polymerization takes place upon addition of ethylene glycol. The heat treatments to obtain the Al_2O_3 and TiO_2 pigment powders were carried out in two stages: initial heating of the resin at 400 °C/1 h (10 °C/min) to pyrolise the organic material, followed by heating at 700 °C/1 h (10 °C/min) to eliminate residual organic material and formation of the crystalline phases. Details of the TiO_2 and Al_2O_3 nanometric pigment powder synthesis are outlined in the flow chart of Fig. 1.

2.2. TiO_2 and Al_2O_3 colored films' deposition by EB-PVD

The TiO_2 and Al_2O_3 colored films were deposited by EB-PVD, using pellets of the pigment powders as target for evaporation. The deposition of films was carried out using an electron beam gun (Telemark-231) operating at 7 kV with beam current of 50 mA. Deposition rates of ~1.0 Å/s were achieved in vacuum of 4×10^{-6} Torr, monitored by a quartz crystal oscillator (Sycon, STM-100). Using this setup we deposited 500–690 nm-thick films on amorphous quartz substrates submitted at 350 °C during the evaporation. The thickness of the films was measured by a Talystep Taylor–Hobson profiler. Tantalum crucibles were used to support the high temperature achieved during the evaporation of the TiO_2 and Al_2O_3 pellets. More details of the EB-PVD system are described in Ref. [20].

2.3. Pigment powders and thick films' characterizations

2.3.1. Structural properties

The crystallinity and phase of the TiO_2/Al_2O_3 pigment powders obtained after the calcination were investigated by

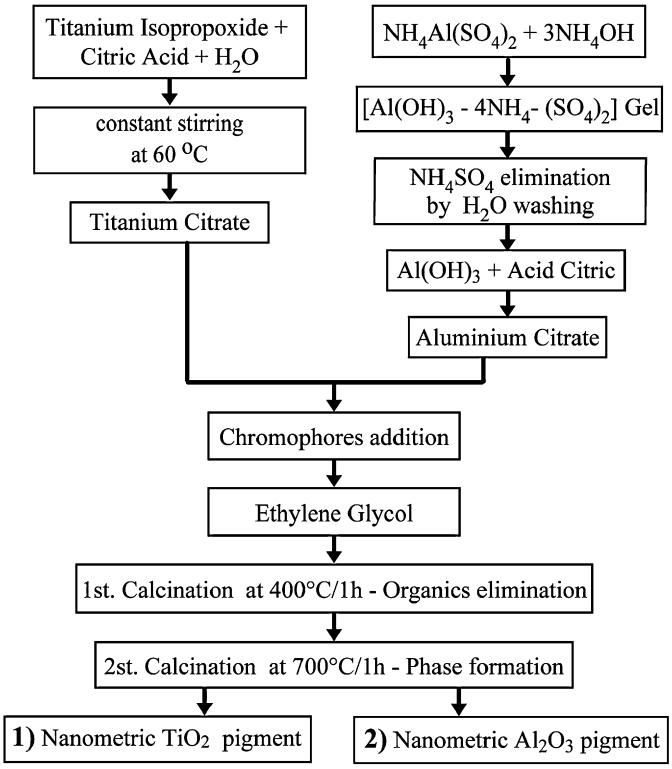

Fig. 1. Flow chart of the TiO_2 and Al_2O_3 nanometric pigments' synthesis, using a modified Pechini's method.

the X-ray diffraction (XRD) technique using a Rigaku Dmax-2500PC diffractometer operating with Cu Kα radiation, with 2θ detector scanning ranging from 20° to 60°, in steps of 0.03°.

2.3.2. Morphological properties

Scanning electron micrographs of the pigment powders were taken by a Zeiss (DSM-940A) Scanning Electron Microscope equipped with field emission gun (SEM-FEG), allowing 100 KX of magnification. The atomic force microscopy (AFM) images were obtained using a Discoverer TMX 2010 microscope from Topometrix. A pyramidal silicon tip with radius of 25 nm was used in all measurements carried out in contact mode. The scan area was 1 × 1 μm consisting of 500 lines scanned at a rate of 2 Hz, to measure the topography, grain size and the surface roughness of the TiO_2 and Al_2O_3 films. The image analysis and average roughness (R_a) measurements were calculated using WSxM 4.0 software from Nanotech Electronica S.L.

2.4. Optical properties

Diffuse reflectance and colorimetric coordinates of the pigments were measured through the Gretac Macbeth Color-eye spectrophotometer 2180–2180UV, in the 350–750 nm range, equipped with standard light sources type A (tungsten lamp, 2800 K), C (halogen lamp, 6775 K), and D50 (day light), following the CIE-$L^*a^*b^*$ colorimetric method recommended by the CIE (Commission Internationale de l'Eclairage) [21]. In this method, L^* is the lightness axis [black (0) → white (100)], b^* is the blue (−) → yellow (+) axis, a^* is the green (−) → red (+) axis, and ΔE is defined as the total color difference ($\Delta E^2 = L^{*2} + a^{*2} + b^{*2}$). UV–Vis transmittance spectra of the colored films were measured in a Cary-17 spectrophotometer in the 200–800 nm range.

3. Results

The most important property to be considered in pigments is the capacity to color the environment in which they are dispersed and make it opaque. The colors obtained for the pigment powders are green (TiO_2:5%Co), brown-reddish (TiO_3:5%Fe), brown (TiO_2:2%Cr), blue (Al_2O_3:5%Co), brown-reddish (Al_2O_3:5%Fe), and light green (Al_2O_3:2%Cr). The pigment powders presented highly homogeneous and accentuated intensity of colors and this effect can be attributed to the nanometric particle sizes. The color of the films deposited by EB-PVD were dark brown (TiO_2:5%Co), brown-reddish (TiO_3:5%Fe), gray (TiO_3:2%Cr), dark brown (Al_2O_3:5%Co), brown-greenish (Al_2O_3:5%Fe) and magenta (Al_2O_3:2%Cr).

Fig. 2a–d shows the FEG-SEM images of the Al_2O_3:5%Co, Al_2O_3:2%Cr, TiO_2:5%Co, and TiO_3:2%Cr nanometric pigment powders, respectively. The resulting pigment powders presented homogeneous morphologic aspects, with average particle size of ∼20 nm. It is observed that although the powders have nanometric particle size, there is a tendency of agglomeration, due to its high superficial energy [22].

Fig. 3a and b presents the X-ray diffraction results for the TiO_2 and Al_2O_3 nanometric pigment powders, respectively, obtained after the two stages of calcinations (as described in Fig. 1). The pigment powders obtained are crystalline and presented single phase, and this confirms the effectiveness of the synthesis method, leading to the crystalline phase formation at low temperatures of calcination.

The TiO_2:5%Co, TiO_2:5%Fe and TiO_3:2%Cr pigment powders (Fig. 3a) presented tetragonal structure (anatase phase), whose space group is $I4_1/amd(141)$, being identified by the index card JCPDS 84–1286. For the Al_2O_3:5%Co, Al_2O_3:5%Fe and Al_2O_3:2%Cr pigment powders (Fig. 3b) was obtained rhombohedral structure (corundum phase), whose space group is $R\bar{3}c(167)$, identified by the index card JCPDS 46–1212.

The crystalline structure of the pigments can be divided into two classes: (1) the materials colored by a mixture of high percentage of other components, which become part of their structure forming new phases, and (2) those which serve as host matrix into which chromophore ions are diluted, such as transition metals, forming a solid solution. In our case, the Co, Cr and Fe chromophore ions were diluted into TiO_2/Al_2O_3 host matrix, substituting the Ti^{4+}/Al^{3+} cations, forming solid solutions without detectable changes in the phase and crystalline structure of the host matrix as observed through the X-ray diffractograms (Fig. 3), yielding high quality pigment powders.

Color is an economical way of creating new interests in an existing product, and also the most noticeable and least

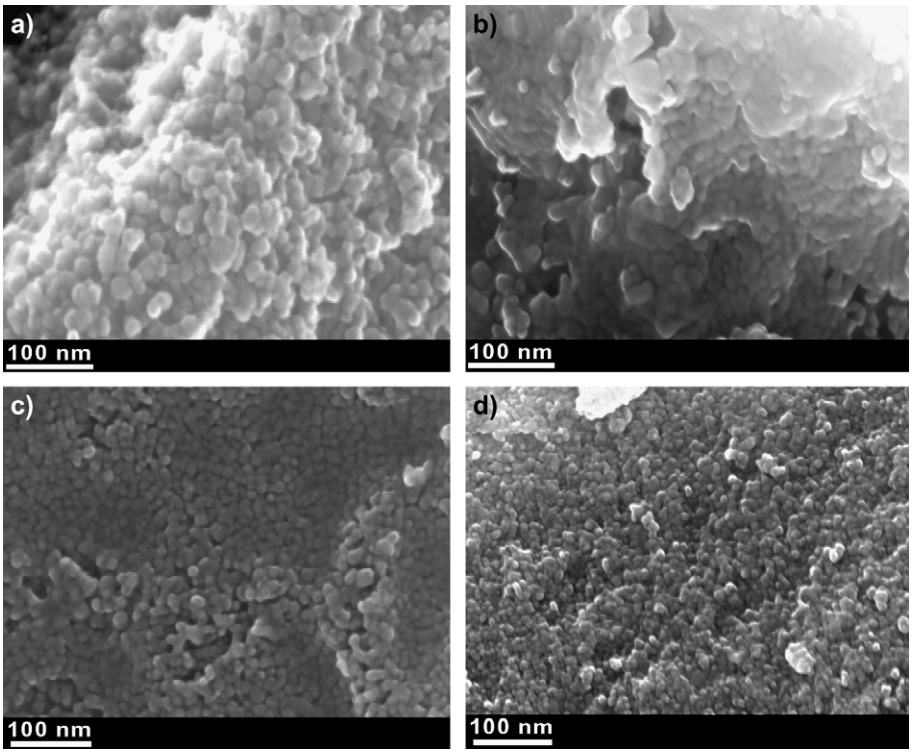

Fig. 2. SEM-FEG images of the nanometric pigment powders: (a) Al_2O_3:5%Co, (b) Al_2O_3:2%Cr, (c) TiO_2:5%Co and (d) TiO_2:2%Cr.

expensive element in decoration. There are several methods for color measurements, but in ceramics the most accepted method to specify the color of a product is the CIE-$L^*a^*b^*$ [21]. This method measures the diffuse reflectance intensity in the visible region to obtain the three colorimetric coordinates L^*, a^*, b^*, obtaining the black/white lightness, green/red and blue/yellow color intensities, respectively, and also the total color difference ΔE. Table 1 presents the colorimetric coordinates (L^*, a^*, b^*) and ΔE for the TiO_2 and Al_2O_3 nanometric pigment powders, for different light sources (A, C and D50).

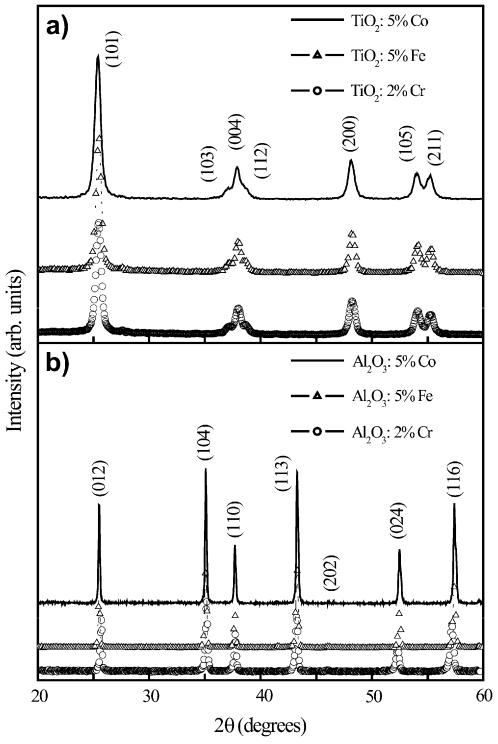

Fig. 3. X-ray diffraction patterns of the nanometric pigment powders after calcination of 700 °C/1 h; (a) TiO_2:5%Co, TiO_2:5%Fe, and TiO_2:2%Cr, and (b) Al_2O_3:5%Co, Al_2O_3:5%Fe, and Al_2O_3:2%Cr.

The TiO_2:5%Co pigment powder (green) showed negative values for a^* (less than −8.00) indicating predominance of green color, and also a low intensity of yellow color (b^* positive values close to 0). The brown-reddish color of the TiO_3:5%Fe pigment powder is evidenced by positive values of a^* (>13) and b^* (>26) colorimetric coordinates, indicating a mixture of red and yellow colors. In the same way, the brown color of the TiO_2:2%Cr pigment is related with the low positive values of a^* and b^* ranging from 2.33 to 7.87. The Al_2O_3:5%Co (blue) presented high negative values of b^* (less than −40.00), indicating intense blue color. The deep brown-reddish color of the Al_2O_3:5%Fe powder is made up of positive values of a^* (>30) and b^* (>35) (more intense compared to the TiO_3:5%Fe). The light green color of the Al_2O_3:2%Cr pigment powder is a sum of light yellow color (b^* values higher than 16) and low intensity of red (a^* values close to 0). The pigments TiO_3:5%Co, TiO_3:5%Fe and Al_2O_3:2%Cr showed more intense lightness values (L^*; black = 0, white = 100) ranging of 45.75, 52.02 and 65.25, respectively, for the light source A. The pigments TiO_3:2%Cr, Al_2O_3:5%Co, and Al_2O_3:5%Fe showed L^* values of 35.12, 28.33, and 37.86 for the light source A, respectively. The low L^* values of these specific pigments can be related with the low diffuse reflectivity intensity

Table 1
Colorimetric coordinates (L^*, a^*, and b^*) and total color difference (ΔE) of the TiO_2 and Al_2O_3 pigment powders, using light sources type A (tungsten lamp, 2800 K), C (halogen lamp, 6775 K), and D50 (day light), following the CIE-$L^*a^*b^*$ standard colorimetric method

Samples	Light source	L^*	a^*	b^*	ΔE
TiO_2:5%Co	A	45.75	−8.85	0.85	46.60
(green)	C	46.83	−13.62	4.80	49.00
	D50	46.66	−12.57	3.69	48.50
TiO_2:5%Fe	A	55.02	16.59	31.20	65.39
(brown-reddish)	C	52.02	13.30	26.96	60.08
	D50	52.68	16.28	27.73	61.71
TiO_2:2%Cr	A	35.12	6.52	7.87	36.58
(brown)	C	39.14	3.42	2.33	39.36
	D50	33.74	6.28	7.01	35.03
Al_2O_3:5%Co	A	28.33	−3.96	−48.11	55.97
(blue)	C	32.64	9.62	−42.36	54.33
	D50	31.29	2.65	−44.05	54.10
Al_2O_3:5%Fe	A	37.86	31.60	43.64	65.85
(brown-reddish)	C	32.82	30.29	35.51	57.06
	D50	33.89	33.45	37.14	60.39
Al_2O_3:2%Cr	A	65.24	4.37	16.60	67.46
(light green)	C	64.23	−1.05	16.60	66.20
	D50	64.52	1.39	16.45	66.60

observed for these samples compared with the others (see Fig. 4a and b).

As stated previously (Section 2.4), the total color difference (ΔE) is a parameter used to compare two samples of the same color (e.g. the total color difference between a standard and a sample). One important information obtained here is that each pigment powder showed very close values of ΔE even for the different excitation light sources A, D50, and C (lamp temperatures of 2800, 5000, and 6775 K, respectively). This result indicates that each pigment will have the same visual color among different types of illumination, which is highly desirable for ceramics.

It is known that the color originates by scattering of light whose wavelengths are complementary to those absorbed by a body. This mechanism involves electron excitation from the valence band to the conduction band under absorption of light. For transition-metal ions (e.g., Co, Fe, Cr) this most commonly occurs with transitions of electrons in the 3d orbital. Electronic transitions that occur in the "color range" are classified into three groups based on the electronic phenomenon causing the transition. These include (1) crystal field transitions, (2) molecular orbital transitions, and (3) color centers. A transition-metal ion can produce various colors depending primarily on the crystal field strength of the host matrix. Besides, the crystal field can be modified due to the lattice distortion caused by the transition metal-ion incorporation and due to the creation of defects (color centers) by charge compensation. In the selection of the host oxide, symmetry of the host cation is of important consideration, since the decrease in the degree of symmetry around the coloring ion enhances the transition probability between 3d orbitals, leading to a deepening of the coloration.

In TiO_2 (anatase), the titanium is hexacoordinated and the addition of the Co^{+2}, Cr^{3+} or Fe^{+3} creates defects such as oxygen vacancies due to the charge compensation. These defects cause a polarization in the titanium, changing the local crystalline field around the chromophore ions, making possible new electronic transitions among distorted 3d orbital levels. These electronic transitions of absorption for the visible spectrum result in the color of the TiO_2:5%Co (green), TiO_2:5%Fe (brown-reddish), and TiO_2:2%Cr (brown) pigment powders. In addition, based on the final color of the synthesized pigment powders, we are considering that the oxidation states of the chromophore ions incorporated into TiO_2 were in majority Co^{+2} ($3d^7$), Cr^{+3} ($3d^3$) and Fe^{+3} ($3d^5$) [12].

Fig. 4a and b displays the diffuse reflectance spectra of the TiO_2 and Al_2O_3 pigment powders in the 350–750 nm region. For the TiO_2:5%Co (green) pigment powder is observed a diffuse reflectance band around 500 nm (with a shoulder at 550 nm) and another broad band of around 700 nm (Fig. 4a). This spectrum is similar to that observed for the Al_2O_3:5%Co (blue) pigment (Fig. 4b) with the position of the bands shifted. The TiO_2:5%Fe (brown-reddish) system possesses an intense and broad diffuse reflectance band from 550 nm to 750 nm. TiO_2:2%Cr pigment powder (brown) has a spectrum very similar to that of TiO_2:5%Fe; however it presents diffuse reflectance with one half of the intensity in the 550–750 nm region.

The diffuse reflectance spectrum of the Al_2O_3:5%Co (blue) (Fig. 4b) presents the characteristic bands of Co^{2+} (electronic configuration $3d^7$). In tetrahedral sites, Co^{2+} causes blue color, as found in some spinels. There is a band around 440 nm (with a shoulder at 500 nm) related to cobalt ion in tetrahedral sites (^2E), and another band at 700 nm that represents the cobalt ion in octahedral sites ($^4T_1$). The Al_2O_3:5%Fe (brown-reddish) (Fig. 4b) presents diffuse reflectance spectrum similar to the TiO_2:5%Fe in the 550–750 nm region, however with less than one half of the intensity. It can be verified for the Al_2O_3:2%Cr (light green) pigment (Fig. 4b) that it presents diffuse reflectance spectrum with increasing intensity from 350 nm to 750 nm and that there are three bands arising at 400 nm, 500 nm and 700 nm, associated with the allowed Cr^{3+} transitions $^4A_2 \rightarrow {}^4T_2$ and $^4A_2 \rightarrow {}^4T_1(F)$ [23,24]. The intensity of these absorption bands depends on the content of the chrome. In the present work, we achieved intense and homogeneous green color for Al_2O_3:2%Cr, using synthesis temperature of 700 °C. Results found by Bondioli and Ferrari [23] showed that alumina presents green coloration only for amounts of Cr^{3+} above 80%.

In Fig. 4c and d is shown the UV–Vis transmittance spectra of the TiO_2 and Al_2O_3 colored films doped with Co, Fe and Cr, respectively. The transmittance of the TiO_2:5%Co and TiO_2:5%Fe films decreases from ~70% at 800 nm to less than ~15% at 400 nm, and this is associated with the properties of high reflectivity and scattering of white light, and also with the high absorbance of the TiO_2 in the UV region. The TiO_2:2%Cr film possesses low transmittance (~20%) in the 800–400 nm region.

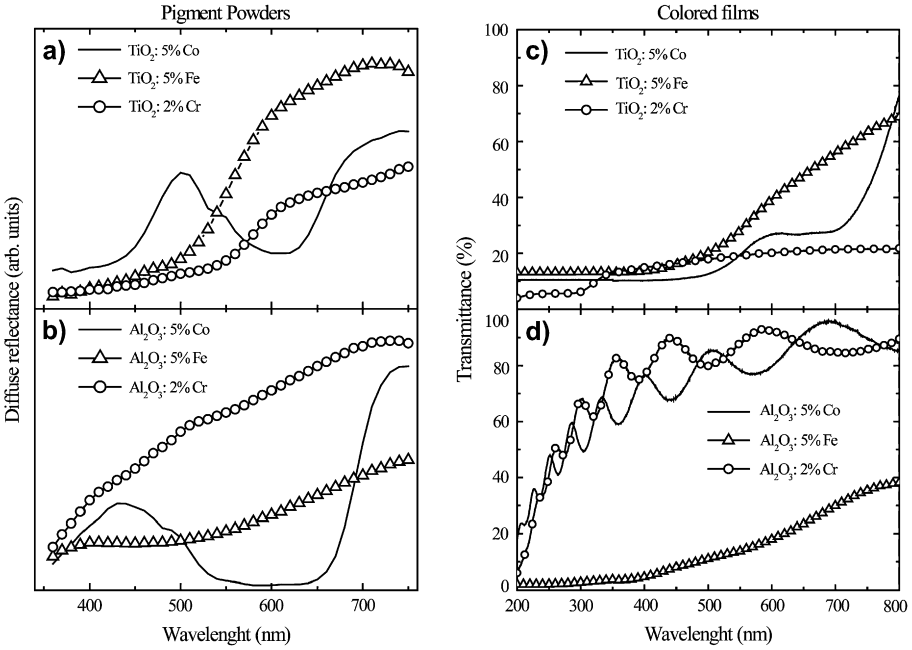

Fig. 4. Diffuse reflectance spectra of the nanometric pigment powders (left): (a) TiO_2 and (b) Al_2O_3; UV–Vis transmittance spectra of the films (right): (c) TiO_2 and (d) Al_2O_3.

Contrarily, the Al_2O_3:5%Co and Al_2O_3:2%Cr films possess high transmittance (90–70%) in the 800–400 nm region, which suddenly decreases (from 70% to 20%) from 400 nm to 200 nm, respectively, due to UV absorption in the band gap region. The Al_2O_3:5%Fe film presented low transmittance, which decreases from 40% to 5% in the 800–400 nm region. Interference fringes due to air–film and film–substrate interfaces were observed in the transmittance spectra of the Al_2O_3:5%Co and Al_2O_3:2%Cr films that presented high transmittance.

The colored film samples of TiO_2:5%Co, TiO_2:5%Fe, TiO_2:2%Cr, Al_2O_3:5%Co, $Al_2O_3$5%Fe and Al_2O_3:2%Cr deposited by EB-PVD presented thicknesses of 580 nm, 520 nm, 440 nm, 690 nm, 400 nm and 500 nm, respectively, measured using a talystep profiler. The films were deposited on amorphous quartz substrates heated at 350 °C during the evaporation process, to improve the adhesion and the packing density of the deposited layer. The thickness of the final film depends on the evaporation time and on the amount of mass pellet that was evaporated.

The study of the optical properties of the colored films was also performed using a method suggested by Peng and Desu [25], which is based on the upper and lower envelopes, T_{max} and T_{min}, respectively, of the interference fringes present in the transmission spectrum at normal incidence in the case of uniform films. The refractive index, n, corresponding to certain wavelengths, λ_i, for which the envelop curves are tangent to the transmission spectrum, were obtained from the following expression:

$$n = \sqrt{N + \sqrt{N^2 - s^2}} \tag{2}$$

where s in the refractive index of the substrate, which was independently obtained [26] for the wavelengths λ_i, the value of N being directly calculated from expression (3):

$$N = 2s\frac{T_{max} - T_{min}}{T_{max} \times T_{min}} + \frac{s^2 + 1}{2} \tag{3}$$

Using the calculated values of n it was also possible to calculate the film thickness, d, using the relationship:

$$d = \frac{a\lambda_i\lambda_f}{2\left(n_i \times \lambda_f - n_f \times \lambda_i\right)}, \tag{4}$$

where a is the number of fringe periods in the $\lambda_i \rightarrow \lambda_f$ interval and $n_i \rightarrow n_f$ are the respective refractive index for the wavelengths. The interference fringes can be describes by the equation $2nd = m\lambda$, where m is the order number, being an integer or half-integer for an upper and a lower (T_{max}, T_{min}) tangent point, respectively.

Fig. 5a and b presents the curves of refractive index as a function of wavelength of the Al_2O_3:5%Co and Al_2O_3:2%Cr thick films, respectively, calculated by the envelope method using Eqs. (2) and (3) as mentioned above. The insets in Fig. 5 show the transmittance spectra and the envelope curves used as basis of the refractive index calculation. The solid points in the insets are the values of T_{max} and T_{min} tangent points, used for the refractive index calculation. It has been found, using the optical characterization method outlined above, that the Al_2O_3:2%Cr film possesses refractive index, n, varying from 1.460 (at 712.3 nm) to 1.540 (at 231 nm), and the Al_2O_3:5%Co film possesses, n, varying from 1.463 (at 690.7 nm) to 1.542 (at 226.4 nm).

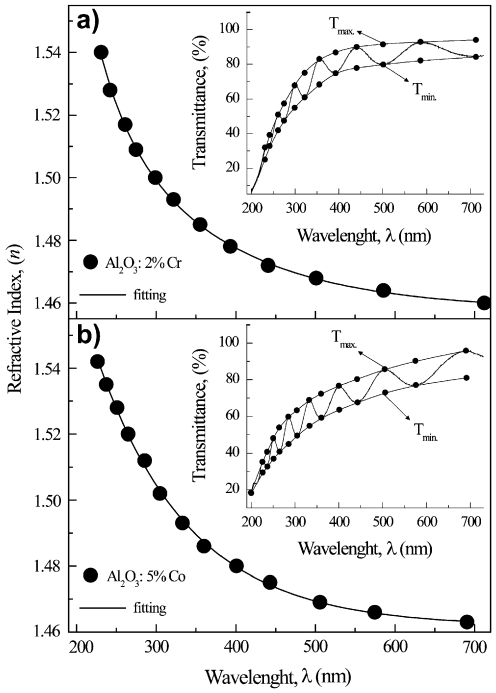

Fig. 5. Refractive index as a function of the wavelength of (a) Al_2O_3:5%Co and (b) Al_2O_3:2%Cr thick-films calculated by envelope method using Eqs. ((2)–(4)) as mentioned in the text. The insets show the UV–Vis transmittance spectra of the films and the envelop curves used as a basis for the calculation. The solid points are the values of T_{max} and T_{min} used for the refractive index calculation.

For comparison purposes, it was reported that films of pure Al_2O_3 have refractive index values of 1.58 (at 1000 nm) and 1.68 (at 250 nm) [27]. Also, electron beam evaporated Al_2O_3 films were reported to possess refractive index value of 1.56 (at 830 nm) measured by ellipsometry [28]. Generally, slight dissociation and oxygen loss occurs during evaporation, and the films grow with a crystalline microstructure with low packing density. The refractive indices are dependent on the degree of oxidation, the substrate temperature and the lattice parameters matching between the substrate and material deposited, affecting the film density achieved.

The values of refractive index obtained for the Al_2O_3 films are slightly below the values reported for pure Al_2O_3 films, probably due to the effects described above and due to the doping with Co^{2+} and Cr^{3+}, which can induce oxygen vacancies in the film structure. To our knowledge, there is no work that reports refractive index results of Co^{2+} and Cr^{3+} doped Al_2O_3 films.

Table 2 summarizes the values of refractive index obtained for the Al_2O_3:5%Co and Al_2O_3:2%Cr thick films, the values of thickness calculated from Eq. (4), and compared with the thickness values measured in the talystep profiler. The difference in the thickness calculated and measured in the talystep profiler for the Al_2O_3:2%Cr ($d_{calc.} = 594$ nm, $d_{measured} = 500$ nm) and Al_2O_3:5%Co ($d_{calc.} = 604$ nm, $d_{measured} = 690$ nm) films is due to the low number of interference fringes in the transmittance spectra (~7 periods of fringes), inducing imprecision in the thickness value calculated. The error in the talystep profiler measurements is ~1.0 nm.

Table 2
Refractive index as function of wavelength for Al_2O_3:2%Cr and Al_2O_3:5%Co, calculated by the envelop method of the transmission spectra

Films			
Al_2O_3:2%Cr ($d_{calc.} = 594$ nm, $d_{measured} = 500$ nm)		Al_2O_3:5%Co ($d_{calc.} = 604$ nm, $d_{measured} = 690$ nm)	
λ (nm)	n	λ (nm)	n
712.3	1.460	690.7	1.463
585.8	1.464	575	1.466
501	1.468	506	1.469
440.6	1.472	443	1.475
393	1.478	401	1.48
355.4	1.485	360.2	1.486
322	1.493	333.2	1.493
299	1.500	305	1.502
274.8	1.509	285.8	1.512
261.2	1.517	264.9	1.52
242	1.528	251	1.528
231	1.54	237.3	1.535
–	–	226.4	1.542

The thickness (d) of the films was also calculated and compared with the value measured in the talystep profiler.
The error for the refractive index (n) calculated from the transmittance spectra by the envelop method is 0.002. The error in (n) has been derived from the values of each standard deviation σ_{n-1}, associated with the fitting parameters of the envelop method, obtained by the least-squares fit.

Fig. 6 show the AFM images of the roughness surface and the grain size of the Al_2O_3:5%Co (Fig. 6a) and TiO_2:5%Co (Fig. 6b). Images obtained on different regions of the samples showed that the films exhibit a homogeneous globular structure. The average dimension of the particles in the initial powders was 20 nm, in the films it was found to be 75 nm (from 50 nm to 100 nm), and the films' average roughness obtained is around 5.5 nm.

4. Conclusions

Nanometric pigment powders of TiO_2:5%Co (green), TiO_3:5%Fe (brown-reddish), TiO_2:2%Cr (brown), Al_2O_3:5%Co (blue), Al_2O_3:5%Fe (brown-reddish) and Al_2O_3:2%Cr (light green) with crystalline phases were obtained at low temperatures of calcination (700 °C/1 h) using a modified Pechini's method. The TiO_2:5%Co, TiO_2:5%Fe and TiO_2:2%Cr pigment powders presented anatase phase (space group: $I4_1/amd$(141), JCPDS 84–1286) while the Al_2O_3:5%Co, Al_2O_3:5%Fe and Al_2O_3:2%Cr pigment powders showed corundum phase (space group: $R\bar{3}c$(167), JCPDS 46–1212). The average particle size of the pigment powders was about 20 nm, measured by SEM-FEG. Each pigment powder presented low color difference (close ΔE values) among the three different types of illumination used (A, 2800 K; D50, 5000 K; and C, 6775 K), evaluated by the measure of the diffuse reflectance spectra and colorimetric coordinates L^*, a^*, b^* using the CIE-$L^*a^*b^*$ method, in the 350–750 nm range.

The colored film samples of TiO_2:5%Co, TiO_2:5%Fe, TiO_2:2%Cr, Al_2O_3:5%Co, Al_2O_3:5%Fe and Al_2O_3:2%Cr deposited by EB-PVD presented thicknesses of 580 nm,

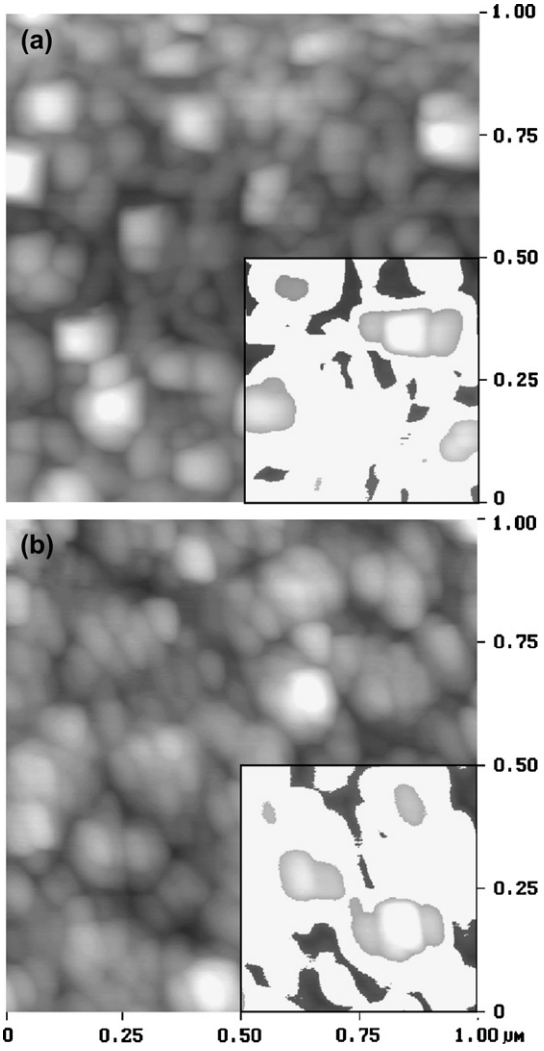

Fig. 6. AFM images of the surface of (a) Al_2O_3:5%Co and (b) TiO_2:5%Co films.

520 nm, 440 nm, 690 nm, 400 nm and 500 nm, respectively, measured using a talystep profiler. The TiO_2 films showed transmittance of 70% at 800 nm decreasing to less than ~15% at 400 nm, associated with the properties of high reflectivity and scattering of white light, and also the high absorbance of the TiO_2 in the UV region. The Al_2O_3:5%Co and Al_2O_3:2%Cr films presented high transmittance at 800 nm (90%) and 400 nm (70%), which suddenly decreases (from 70% to 20%) from 400 nm to 200 nm (band gap region). The Al_2O_3:5%Fe film presented low transmittance, which decreases from 40% to 5% in the 800–400 nm region.

Transmission spectra envelop method has been used to obtain refractive index and thickness of the Al_2O_3 colored thick films. The Al_2O_3:2%Cr film possesses refractive index varying from 1.460 (at 712.3 nm) to 1.540 (at 231 nm), and the Al_2O_3:5%Co film possesses refractive index varying from 1.463 (at 690.7 nm) to 1.542 (at 226.4 nm). AFM images obtained on different regions of the Al_2O_3:5%Co and TiO_2:5%Co samples showed that the films exhibit a homogeneous globular structure. The average grain size obtained for the films is around 75 nm and the average roughness is ~5.5 nm.

Acknowledgements

The authors gratefully acknowledge the financial support of the Brazilian financing agencies FAPESP, CNPq, PRONEX/FINEP and CAPES.

References

[1] Weber IT, Maciel AP, Lisboa-Filho PN, Longo E, Leite ER, Paiva-Santos CO, et al. Nano Lett 2002;2(9):969–73.
[2] Bernardi MIB, Cava S, Paiva-Santos CO, Leite ER, Paskocimas CA, Longo E. J Eur Ceram Soc 2002;22(16):2911–9.
[3] Maciel AP, Lisboa-Filho PN, Leite ER, Paiva-Santos CO, Schreiner WH, Manietti Y, et al. J Eur Ceram Soc 2003;23(5):707–13.
[4] Feldmann C. Adv Mater 2001;13(17):1301–3.
[5] Xie Y, Yuan C. Mater Res Bull 2004;39(4–5):533–43.
[6] Yin S, Fujishiro Y, Wu J, Aki M, Sato T. J Mater Process Technol 2003;137(1–3):45–8.
[7] Watson SS, Beydoun D, Scott JA, Amal R. Chem Eng J 2003;95 (1–3):213–20.
[8] Campostrini R, Ischia M, Palmisano L. J Therm Anal Calorim 2004;75(1):13–24.
[9] Phani AR, Santucci S. Mater Lett 2001;50(4):240–5.
[10] Wang J, Una S, Klabunde K. J Appl Catal B Environ 2004;48(2):151–4.
[11] Di Paola A, Garcìa-Lòpez E, Ikeda S, Marci G, Ohtani B, Palmisano L. Catal Today 2002;75(1–4):87–93.
[12] Carp O, Huisman CL, Reller A. Prog Solid State Chem 2004;32 (1–2):33–177.
[13] Pati RK, Ray JC, Pramanik P. Mater Lett 2000;44(5):299–303.
[14] Chen G, Rühle M. Surf Coat Technol 2005;191(2–3):263–6.
[15] Ichinose N. Superfine particle technology. London, UK: Springer-Verlag; 1993.
[16] Pechini M. P. US Patent 3303697; 1967.
[17] Quinelato AL, Longo E, Leite ER, Bernardi MIB, Varela JA. J Mater Sci 2001;36(15):3825–30.
[18] Pontes FM, Longo E, Rangel JH, Bernardi MIB, Leite ER, Varela JA. Mater Lett 2000;43(5–6):249–53.
[19] Kakihana M, Arima M, Nakamura Y, Yashima M, Yoshimura M. Chem Mater 1999;11(2):438–50.
[20] De Vicente FS, Rubo EAA, Li MS. Revista Brasileira de Aplicações de Vácuo 2004;23(1):11–6.
[21] CIE. Recommendations of uniform color spaces, color difference equations, phychometrics color terms. Supplement no.2 of CIE Publ. No. 15 (E1–1.31) 1971, Bureau Central de la CIE, Paris; 1978.
[22] Grosa JR. Nanostruct Mater 1999;12:987–92.
[23] Bondioli F, Ferrari AM. J Am Ceram Soc 2000;83(8):2036–40.
[24] Mariotto G, Montagna M, Rossi F. Phys C – Solid State Phys 1986;19(16):3029–37.
[25] Peng CH, Desu SB. J Am Ceram Soc 1944;77(4):929–38.
[26] Malitson IH. J Opt Soc Am 1965;55(10):1205–65.
[27] Eriksson TS, Hjortsberg A, Niklasson GA, Granqvist CG. Appl Opt 1981;20(15):2742–6.
[28] Schubert EF, Passlack M, Hong M, Mannerts J, Opila RL, Pfeiffer LN, et al. Appl Phys Lett 1994;64(22):2976–8.